Biosensors and Bioelectronics 25 (2009) 759–766

Contents lists available at ScienceDirect

Biosensors and Bioelectronics

journal homepage: www.elsevier.com/locate/bios

Whole cell biosensing via *recA::mCherry* and LED-based flow-through fluorometry

R.L. Martineau[a,c,*], V. Stout[b], B.C. Towe[a]

[a] Harrington Department of Bioengineering, P.O. Box 879709, Arizona State University, Tempe, AZ 85287-9709, USA
[b] School of Life Sciences, P.O. Box 874501, Arizona State University, Tempe, AZ 85287-4501, USA
[c] Center for Ecogenomics, The Biodesign Institute, 1001 S. McAllister Avenue, Arizona State University, Tempe, AZ 85287-6501, USA

ARTICLE INFO

Article history:
Received 10 June 2009
Received in revised form 14 August 2009
Accepted 15 August 2009
Available online 2 September 2009

Keywords:
Whole-cell biosensor
Green fluorescent protein
Red fluorescent protein
mCherry
Escherichia coli
Light-emitting diode

ABSTRACT

A miniature flow-through optical cell has been developed with the potential for integration into a stand-alone, potentially disposable whole-cell biosensor platform. The compact and inexpensive optical system is comprised of closely coupled light-emitting diodes (LEDs), light-to-frequency (LTF) photodiodes, and celluloid filters. The system has been optimized to measure fluorescent reporters produced by cultures of biosensor cells in liquid suspension. As demonstration subjects, *Escherichia coli* cells carrying medium-copy plasmids with fluorescent reporter fusions to the *rec* promoter were exposed to the DNA-damaging agent mitomycin C (MMC). As reporter proteins, green fluorescent protein (GFP) and red fluorescent protein (RFP) were compared for suitability in the compact instrument. The RFP mCherry outperformed GFP (GFPmut3.1) as a reporter protein in the developed system on two counts. First, measurement distortions due to high optical density suspensions are minimal using RFP compared to GFP. Second, the limit of detection for MMC is estimated at 0.25 nM for *recA::mCherry* and 2.0 nM for *recA::gfpmut3.1*. Finally, a measurement method is presented whereby multiple channels of optical data are calibrated in an integrated fashion to allow simultaneous measurement of fluorescence and biomass concentration. The method substantially eliminates optical distortions due to dense samples and thus obviates the conventional need for sample dilution prior to measurement.

1. Introduction

An important class of whole-cell biosensors takes advantage of the diverse genetic responses of bacteria to environmental stresses (LaRossa and Van Dyk, 2000). In general, induction of reporter proteins can be correlated to activation of a stress-responsive promoter and by extension to the presence of the analyte of interest. Numerous stress-inducible promoters have been identified, cloned, and coupled to reporter proteins of various modalities to enable biologically-responsive and relevant sensor systems (Belkin, 2003; Daunert et al., 2000; Lei et al., 2006; Ron, 2007; Yagi, 2007). To date, whole-cell biosensors have been developed with sensitivity to mutagens, heavy metals, phenols, naphthalene, toluene, ammonia, methane, and various biologicals (Yagi, 2007). Applications that stand to gain from improved whole-cell biosensing technology include air and water quality assessment, bio-warfare defense, drug screening, chemical mutagenicity assessment, and space biology and hazard assessment.

A key element to a promoter-based whole-cell biosensor is the reporter protein. Many different reporter proteins have been investigated for use in whole-cell biosensors (Daunert et al., 2000). Optical reporters figure prominently in modern implementations, with bioluminescence-based reporters being especially popular due to their excellent sensitivity and response time (Bulich et al., 1996; Gu and Gil, 2001; King et al., 1990; Lee et al., 2005; Simpson et al., 1998; Van Dyk et al., 2001). Fluorescence-based reporters, including green fluorescent protein (GFP) and its many spectral variants, have also been popular despite a lower sensitivity and a longer response time (Baumstark-Khan et al., 2001; Hakkila et al., 2002; Justus and Thomas, 1999; Kostrzynska et al., 2002; Norman et al., 2005; Rabbow et al., 2003).

Despite the drawbacks of fluorescent proteins as reporters, they do offer important advantages, especially when considering remote deployment in portable systems. Most notably, fluorescent proteins can be highly stable once formed, and can exhibit half-lives of days. One result of this is the de-coupling of the event transduction (promoter activation) and the event detection (fluorescence readout) such that sensor strains can be exposed to hazards and then, even days later, have fluorescence measurements taken. This feature of

* Corresponding author at: Center for Ecogenomics, The Biodesign Institute, 1001 S. McAllister Avenue, Arizona State University, Tempe, AZ 85287-6501, USA. Tel.: +1 480 232 6684.
E-mail addresses: Rhett.Martineau@gmail.com (R.L. Martineau), VStout@asu.edu (V. Stout), Bruce.Towe@asu.edu (B.C. Towe).

0956-5663/$ – see front matter © 2009 Elsevier B.V. All rights reserved.
doi:10.1016/j.bios.2009.08.042

course makes fluorescent reporters suitable for some applications (dosimetry, for instance) but not others (warning systems). Additionally, a long half-life enables reporter protein accumulation over time which can be helpful in detecting weak promoter activation. In fact, accumulation of fluorescent reporters over extended durations can result in sensitivities comparable to those achieved via bioluminescence (Justus and Thomas, 1999; Sagi et al., 2003). Furthermore, extreme reporter stability is advantageous when remote sensing systems may be subject to harsh or variable operating conditions.

Fluorescent reporters have responded well to iterative improvements. Thus, through both biological engineering and the obtaining of novel substrates, the palette of available fluorophores has greatly expanded. Species exist with emissions spanning the visible spectrum (Shaner et al., 2005). Of particular note for this work are the red fluorescent proteins (RFPs), and numerous works have been successful toward their isolation and improvement (Bevis and Glick, 2002; Campbell et al., 2002; Shaner et al., 2004; Shrestha and Deo, 2006; Sörensen et al., 2003; Wiedenmann et al., 2005). As reporters in whole-cell biosensors, RFPs offer especially attractive features including lower optical interactions with cellular media and lower excitation energy.

Typically, luminescence from reporter proteins in cell suspensions is measured using instrumentation systems based on photomultiplier tubes (PMTs), high-power excitation sources, and complex optics and grating mechanisms. These systems are not ideal for remote or distributed applications, however, due to their bulkiness, high-energy consumption, high-voltage operation, and instability in the face of physical perturbations. Detector systems comprised of light-emitting diodes (LEDs), silicon photodetectors (PDs), and fixed filters, on the other hand, are more practical for remote applications due to their robustness to mechanical perturbations, small size, and low power requirements. Compact optical detectors have been built using low-power LEDs and PDs, with sensitivity suitable for analytical instruments, and continuous improvements to LEDs and PDs will make them even more attractive in the future (Dasgupta et al., 2003; Gotz and Karst, 2006).

With an aim towards portability, this work develops a whole-cell biosensor system consisting of compact optical hardware and fluorescent *Escherichia coli* cells. Optical components include light-emitting diodes, celluloid filters, and light-to-frequency (LTF) photodiodes (PDs). The optical system can potentially be integrated into a stand-alone platform for automated, remote biosensing applications. Alternatively, the device can be used as a portable measurement system, where a user collects whole-cell samples from a sensing location and injects them into the detector flow path.

The optical system has been designed for simultaneous detection of green fluorescence, red fluorescence, and cell biomass concentration. *E. coli* cells have been engineered to serve as sensor elements for DNA damaging agents. Both a GFP (gfpmut3.1, (Cormack et al., 1996)) and an RFP (mCherry, (Shaner et al., 2004)) are used to report the activity of the well-characterized SOS promoter, *recA*.

2. Methods

2.1. Instrumentation

2.1.1. Optical design

High-brightness LEDs were combined with light-to-frequency silicon PDs to enable the pseudo-simultaneous detection of fluorescence (either red or green) and cellular biomass via 90° scatter. Simple celluloid filters, despite their relatively broad optical cut-offs, have been used to condition the light at both the excitation and emission legs of the optical cell due to their low cost and low bulkiness.

2.1.1.1. Mechanical design. A strategy of close coupling of the excitation sources, filters, sample chamber, and detectors was adopted for this work to reduce the optical component count and complexity, thus facilitating compact and cost-effective instruments. See Fig. 1. Filter sets and excitation sources were chosen to maximize the signal light to background light ratio, while retaining sufficient throughput. In general, the shallow cut-offs of the celluloid filters combined with the wide excitation beams of the LEDs necessitated off-peak excitation.

Chassis components were milled from black acetal (Delrin^{TM}) and the sample chamber in transparent acrylic. The sample chamber measured roughly 3 mm × 4 mm × 8 mm, machined and polished with a wall thickness of approximately 0.3 mm for a sample volume of approximately 95 μl. To control light passage through the chamber and to reduce unwanted scatter, a mask of black paint was applied to create an optical aperture measuring approximately $1 \times 3\,mm^2$.

2.1.1.2. Optical multiplexing. The ability to probe a sample for red fluorescence, green fluorescence, and biomass-dependent scatter was achieved by alternating the active pair of LED and filter-covered PD. Green fluorescence was measured using a 444 nm blue LED (Roithner-Lasertechnik, LED450-06U) conditioned with a blue filter (Rosco, Inc. #346) which coupled to a PD through a yellow filter (#12); red fluorescence was excited with a 522 nm green LED (Kingbright L7113VGC/H) conditioned with a green filter (#389) and measured with a red (#26) filter-covered PD; cell biomass was assayed using scattered excitation light from the green LED as measured by the yellow filter-covered PD.

LEDs and PDs were interfaced to a personal computer (PC) and data acquisition card (DAQcard 6024E, National Instruments) via a custom printed circuit board. Sampling protocols and data were managed using LabVIEW software (National Instruments) run on the attached PC. See supplementary material for a photograph of the device.

LEDs were alternately pulsed for approximately 1 s. LTF PDs (TSL237S, TAOS Inc.) produced digital pulse trains which were coupled to the input lines of a digital multiplexer. Selector signals from the PC were used to enable the appropriate channel of the digital multiplexer in order to pass the appropriate detector's signal to the counter on the data acquisition board.

Samples were manually injected into the detector's flow path. In general, five measurements were taken and averaged for each injected sample.

2.2. Biological components

2.2.1. Bacterial strains

Routine genetic work was done using DH5α cells (Invitrogen). All final plasmid constructs were transformed into DJ480 cells (Majdalani et al., 2005). DJ480 cells are based on *E. coli* MG1655 with Δ(argF-*lac*)U169. Phenotypically, DJ480 cells are *lacI*$^-$ but *recA*$^+$.

2.2.2. Plasmid construction

pTrc99a was used as the plasmid basis for the sensors in this work (Amann et al., 1988). pTrc99a is an expression vector characterized by an ampicillin resistance marker, a medium copy origin of replication, a LacI-repressible promoter with a multiple cloning site and strong transcription terminator, and a constitutively-expressed *lacI*.

Inducible constructs were created by combining pTrc99a components with the *recA* promoter amplified from MG1655 lysates (see supplementary material). Primers for the reaction were based on published primers (Norman et al., 2005) but were modified to produce 5′ *XhoI* and 3′ *NcoI* sites. The resulting

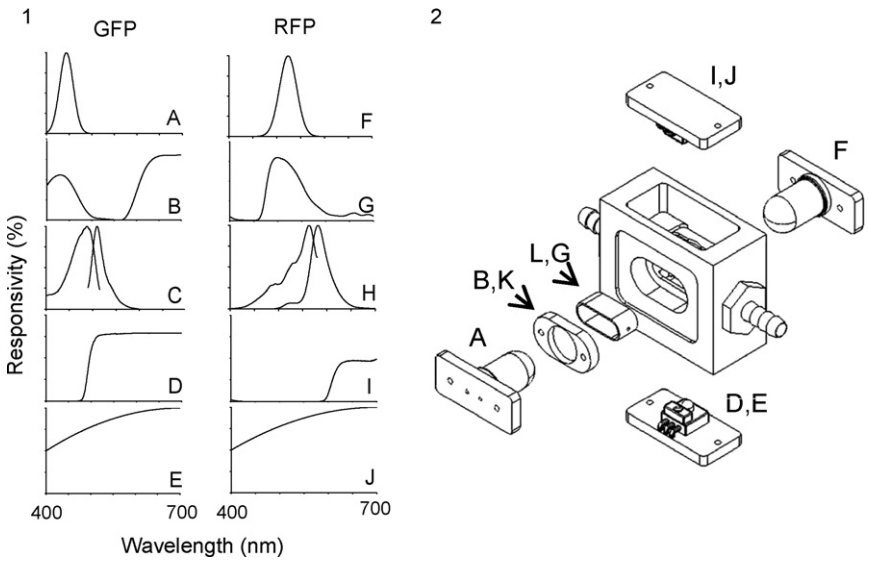

Fig. 1. Optical setup. Off-peak excitation and close-coupling of the optical components enables high-sensitivity detection in a cost-effective package. Filters were chosen in a manner that maximizes the signal light to background light ratio. The optical characteristics of GFP detection components are shown in panel 1: (A) a blue LED passes light through an excitation filter (B); (C) the absorbance spectrum of GFP is shown to the left of its emission spectrum; (D) the pass-band of the emission filter; (E) the spectral responsivity of the light-to-frequency detector. The optical train for RFP detection is shown in the center panel. In panel 2, the physical placement of the components is shown in an exploded view. Filters were affixed directly to the sample chamber lid (K), sample chamber floor (G), and the photodetectors (E and J).

amplicon was digested and ligated to a second fragment, the amplicon of a PCR reaction of pTrc99a consisting of the region between the MCS and *lacI* gene. The resulting plasmid consisted of the *recA* promoter with downstream multiple cloning site, the *rrnBT1T2* transcription terminator, ampicillin resistance gene, and pBR322 *ori*. Genes for GFP (*gfpmut3.1*) and RFP (*mCherry*) were subsequently PCR-amplified and inserted under *recA* control to produce plasmids pRM124 (*recA::gfpmut3.1*) and pRM125 (*recA::mCherry*).

Constitutive constructs were created by modifying the *tac* promoter of pTrc99a at two points. The first mutation disrupted repressor binding by altering the LacI binding sequence. The second mutation altered the -10 region of the promoter, matching it to the *E. coli* consensus sequence. Reporter genes were inserted to create plasmids pRM104 (constitutive *gfpmut3.1*) and pRM105 (constitutive *mcherry*). The modified plasmid without a reporter gene insert was designated pMB99a.

All plasmids were verified by sequencing and transformed into DJ480 cells.

It is worth noting that in addition to the reporters already mentioned, one other GFP (acGFP1, Clontech) and two other RFPs (dsRed2 and dsRedM, both from Clontech) were tested as reporters in the various plasmids. However, only *gfpmut3.1* and *mcherry* proved functional in all expression paradigms and were thus selected out of necessity and not for any other feature.

2.3. Cell culture

Neidhardt EZ-Rich Medium (Teknova, CA) was used for all experiments, supplemented with 100 μg/ml ampicillin. Neidhardt medium enables a very fast growth rate while preserving optical clarity.

Each experiment was started by streaking Neidhardt plates with cells from frozen stock, cultured overnight. A single colony was then placed on liquid Neidhardt and again incubated overnight. Overnight incubations were done at 37 °C and shaken at approximately 50 rpm on a 10 in. radius disc rotary mixer. Aliquots of overnight culture were diluted 1:100 in fresh media in triplicate and supplemented with experimental treatments.

2.4. DNA-damage induction

RecA is a key component of the SOS regulon, and *recA* promoter activity increases as a result of single-stranded DNA (ssDNA) accumulating in the intracellular spaces (Snyder and Champness, 2003). ssDNA accumulates when cellular repair mechanisms act on damaged sections of DNA. Thus, *recA* activity can be correlated to the concentration of DNA damaging agents to which cells are exposed.

Mitomycin C (MMC) is a model DNA-damaging agent which has been extensively used in whole-cell sensor studies (Gu and Gil, 2001; Kostrzynska et al., 2002; Kuang et al., 2004; Polyak et al., 2001; Quillardet et al., 1982; Wei et al., 2001). MMC was used in this work to facilitate comparisons with previous studies. Cells were exposed to various concentrations of MMC, and the effect of those doses on the *recA* promoter was inferred by quantifying the production of fluorescent reporters. In general, higher doses of MMC produce higher *recA* promoter activities and correspondingly higher concentrations of reporter proteins, as measured by an increase of fluorescence.

A 15 mM mitomycin C stock solution was prepared by adding 1 mL of a 90% propylene glycol solution to 5 mg mitomycin C powder (Sigma–Aldrich). Propylene glycol solutions have been observed to retain 100% MMC activity for up to 6 months when stored at 4 °C (Paborji et al., 1993). For each experiment, mitomycin C was freshly prepared by diluting the propylene glycol stock 1:50 to 300 μM using sterile water. Overnight cultures were diluted into fresh media dosed with aliquots of MMC. Cells were then allowed to grow for 24 h in a rotary shaker at 37 °C before fluorescence measurements were taken.

2.4.1. Induction factor

When optical whole-cell biosensors are used to assess the potency of DNA-damaging agents, the induction factor, F_i, is commonly used:

$$F_{\mathrm{i}} = \frac{F_{\mathrm{s}}/OD_{\mathrm{s}}}{F_0/OD_0} \quad (1)$$

Here, F_{s} represents the fluorescence intensity of a sample at a given treatment level in relative fluorescence units, OD_{s} represents that

sample's optical density at a given wavelength, and F_0 and OD_0 represent the corresponding measurements for an untreated sample. A treatment level that produces an induction factor of 2 is commonly defined as an assay's limit of detection (Kostrzynska et al., 2002; Norman et al., 2005).

2.4.2. Fluorescence signal to noise ratio

In this work, the biosensor limit of detection is also estimated using the signal to noise ratio (SNR). Signal to noise ratio was computed by taking the difference between the averages of three trials at a given treatment level from three untreated samples, dividing by the standard deviation at that treatment level. The lowest treatment eliciting a signal to noise ratio of 3 was reported as the assay limit of detection.

3. Results

3.1. Fluorescence response to MMC

Cells carrying both pRM124 (*recA::gfpmut3.1*) and pRM125 (*recA::mCherry*) plasmids were exposed to 10-fold dilutions of MMC. 0, 0.1, 1, and 10 nM treatments of MMC were administered three times on separate days using distinct starter CFUs, in triplicate for each experiment. Higher doses were also administered, up to 1000 nM, in triplicate, but not for all experiments. After 24 h incubations, cultures were sampled directly by injecting undiluted, untreated samples into the flow-path of the detector. The resulting fluorescence induction factors are shown in Fig. 2 below.

The fluorescence responses were fit to the following expression:

$$F(c) = \frac{F_{\max} - F_0}{1 + ke^{\log c}} + F_0 \quad (2)$$

where fluorescence induction factor, F, unit-less, is expressed as a function of MMC concentration, c, in nM. $F_{\max}$ denotes the saturating fluorescence induction value observed for the system, F_0 the fluorescence induction factor at the baseline treatment level, and k and r are constants determined through the curve fit procedure.

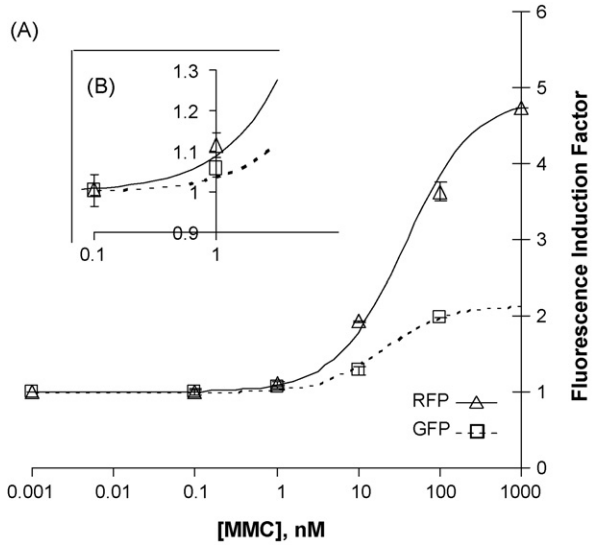

Fig. 2. MMC response of *recA* biosensors in an LED/LTF fluorometer. In A, the results of exposing *recA* biosensors to increasing doses of MMC are plotted for both *recA::mCherry* (△) and *recA::gfpmut3.1* (□) cells. Results are from experiments on three separate days, where each experiment was performed in triplicate. Computing fluorescence induction results in high day-to-day repeatability and a good curve fit. In general, higher signal to noise ratios are observed for MCherry-based biosensors than for GFPmut3.1-based biosensors in the LED/LTF fluorometer. The data for the 1 nM treatment level are shown on a finer scale in B.

The procedure entailed linearizing the above expression and fitting the results using a least-squares method. The resulting curve fits are shown as the dashed lines in Fig. 2.

3.1.1. Whole-cell sensor performance

Responsiveness to MMC is detectable over 4 orders of magnitude using *recA::mCherry*. GFP cells show responsiveness over only 3 orders of magnitude, due to a low signal to noise ratio at the lower concentrations. mCherry carriers responded with a higher peak induction factor, roughly 5 compared to the peak of about 2 for GFP carriers.

3.1.2. Assay limit of detection

Both the 2-fold induction and SNR of 3 criteria are used to report the limit of detection for both the *recA::mCherry* and *recA::gfpmut3.1* constructs in DJ480 cells. For *recA::gfp* cells in DJ480, as measured using the flow-cell fluorometer of this work, the limit of detection is estimated at 2.0 nM and more than 100 nM MMC for the SNR of 3 and 2-fold induction methods, respectively. For *recA::mCherry* cells in DJ480, as detected in the flow-cell fluorometer of this work, the limit of detection is estimated at 0.25 nM and 11.7 nM MMC for the SNR of 3 and 2-fold induction methods, respectively. By either LOD estimation method, a nearly 10-fold difference in achievable limit of detection is observed between the GFP and RFP constructs.

3.2. High-density fluorescence and OD estimation

Since all samples were administered directly to the optical detector without dilution or processing, the effect of high optical density on fluorescence induction measurement needed to be characterized. The effect of high sample density is known to affect both optical density measurement and fluorescence measurement. For moderately dense samples, the relationship between biomass and optical density is non-linear, with high density sample biomass being underestimated by optical density measurements. Fluorescence signals are also subject to complications from highly dense samples, due to self-shielding. Fluorescence measurements are further complicated since they are commonly normalized to optical density.

Although standard lab practice is to simply dilute samples before optical measurements, for remote applications dilution may be inconvenient. Thus, an approach was developed whereby both fluorescence and biomass concentration were concurrently estimated in undiluted samples. This was possible using a set of equations whose solution resulted in the estimation of the interacting unknown parameters. First, the approach to high-density estimation using GFP-based sensors is presented in detail. Next, the method is applied to RFP sensors and the results are compared.

3.2.1. Modeling GFP and OD optical interactions

It was assumed that a two-equation system could be found to enable the simultaneous and coupled determination of the sample's cell concentration and percentage fluorescence. Each equation modeled a detectors' response to an administered sample, and measurements taken from that pair of detectors provided sufficient information to solve the system and estimate the two unknown components of the sample. From preliminary observations it was known that the amount of GFP in the sample significantly affected the readings of the OD sensor, and vice-versa. Additionally, the response of the cell biomass sensor had been observed to best fit a third order polynomial. Thus, a system of two equations was sought where each detector's response was a function of the two measurements with unknown interactions, up to a third order response. Each detector's response was assumed to fit a standard third order linear response equation which could be parameterized according

to standard statistical methods (Montgomery, 2005):

$$y_1 = \alpha_0 + \sum_{i=1}^{n}\alpha_i x_i + \sum_{i=1}^{n}\alpha_{ii}x_i^2 + \sum_{i=1}^{n}\alpha_{iii}x_i^3 + \sum\sum_{i<j}^{n}\alpha_{ij}x_i x_j + \sum\sum_{i\neq j}^{n}\alpha_{iij}x_i^2 x_j + \varepsilon_0 \quad (3)$$

where y_1 represents the fluorescence detector response in Hz, x_1 and x_2 represent the percentage GFP fluorescence and the OD_{620} value of the sample, and the α terms represent the effect coefficients for the GFP sensor for each main factor or interaction term. A second equation similar to that above was assumed for the cell biomass sensor, using β terms for effect coefficients.

Significant terms in the model above, as well as their coefficients, were determined using a commercial statistics package (Design Expert 6.0). A battery of cell mixtures and densities were administered to the detector. One constituent of the mixture consisted of DJ480 cells containing the plasmid for constitutive GFP production. The other constituent consisted of DJ480 cells with a matching plasmid without any reporter insert. Samples for calibration were first prepared by culturing each cell type overnight in Neidhardt EZ-Rich medium (Teknova, CA), followed by dilution with blank media to OD_{620} of 2.1. Cells were probed for optical density at 620 nm. Mixtures of fluorescent/non-fluorescent cells were then prepared by adding volumetric ratios to match the desired percentage fluorescence treatment values. That is, the 100% GFP treatment consisted of a cell suspension consisting entirely of GFP-expressing cells; a 25% GFP treatment consisted of 25% GFP-expressing cells and 75% non-expressing cells. These high-OD mixtures were then serially diluted in 2-fold decrements. The range of fluorescence percentages spanned from 0% to 100% with five treatments, and the overall cell densities ranged from 0.1 to 2.1 OD_{620} units (measured directly in a benchtop spectrophotometer without sample dilution), also with five treatments. The experimental design is summarized in Table 1.

Coefficients for the models were determined by successive regeneration of the fitting parameters and determination of statistically valid terms, starting with the highest order terms and progressing downward. The term coefficients are shown at right in Table 1.

Given the light intensities registered on the photodetectors for a given sample, the solution of the two response equations estimates the cell density and the percentage fluorescence. This approach enables the direct sampling of undiluted overnight cultures of variable constituency, without any need for sample pre-processing or manipulations.

Table 1
Simultaneous GFP and OD model parameters.

Natural variables		Responses		Coefficients			
% GFP	OD_{620}	y_1	y_2	α	Value	β	Value
50	1.1	30	2931	α_0	32.12	β_0	3015.28
50	0.1	3	211	α_1	10.85	β_1	81.29
50	2.091	91	8955	α_2	32.98	β_2	2328.16
50	1.102	33	3010	α_{11}	–	β_{11}	−13.66
50	1.097	32	2997	α_{12}	−17.73	β_{12}	−483.10
14	1.809	43	6170	α_{22}	−20.22	β_{22}	146.25
100	1.095	47	3091	α_{111}	–	β_{111}	–
50	1.096	32	2998	α_{112}	–	β_{112}	–
85	1.808	85	6541	α_{221}	27.86	β_{221}	590.23
0	1.108	17	2906	α_{222}	19.04	β_{222}	868.60
85	0.389	16	1089				
50	1.094	33	3110				
14	0.392	8	871				

In Fig. 3, the result of the coupled response surfaces approach to GFP measurement is compared with the simpler method of normalizing the fluorescence signal to the biomass signal.

3.2.2. System solution and component estimation

For undiluted samples, the two-equation approach to GFP estimation is more accurate than the simpler method of normalizing the fluorescence intensity to optical density. The comparison is shown in Fig. 3. In Fig. 3A, an improvement in accuracy is apparent. A similar plot for cell biomass estimation was created, but is not shown here.

Additionally, calibration of the detectors in this manner demonstrates that highly dense samples distort the dose response curves. For the data presented in 3B, *recA::gfp* cells were exposed to 10-fold increases in MMC concentration. For the upper curve, the two-equation method was applied, and the fluorescence induction factor was computed based on the estimated fluorescence content. The bottom curve was created by computing the induction factor using fluorescence intensity signals normalized by the online, raw cell biomass signal. Note especially that if an induction factor of 2 criteria is applied to the data, the direct normalization method will require a much higher MMC concentration to cross the threshold.

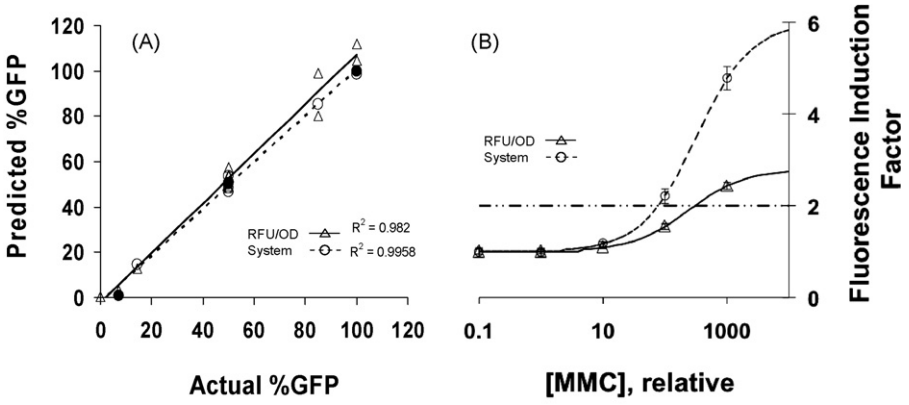

Fig. 3. GFP estimation in turbid cultures. In A, GFP is estimated in mixed samples by two methods. First, fluorescence intensities are normalized by the detector's biomass signal and then fit to a simple curve (△). The correlation to actual GFP content is then displayed. In the second case, the interaction effects of GFP and cell biomass are explicitly accounted for using a system of equations. Both samples used to create the model (○) and others not used to create the model (●) are shown in correlation to the actual GFP content of the samples. Optical densities of the assayed samples ranged from 0.1 to over 2.0, as measured directly at 620 nm. In B, the inner filter effect on fluorescence intensity in high-density samples is illustrated. In one case, the raw fluorescence signal is normalized to the raw biomass signal, and an induction factor is computed (△). In the other, the two-equation interactions model is used to estimate the percentage GFP and the induction factor computed (○). When the optical attenuations are accounted for in the interactions model, a more accurate and pronounced fluorescence induction is identified.

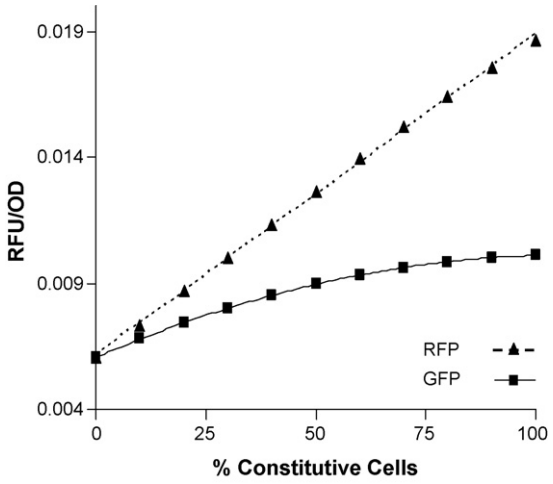

Fig. 4. Optical distortions of mCherry and GFPmut3.1. Response equations were fit to data with mixtures of dark and either constitutive GFP or RFP cells. Then, the predicted biomass-normalized fluorescence quantities were plotted as a function of % constitutive cells. A linear response is observed for increasing RFP-containing cells (▲), whereas a diminishing response is observed using GFP-expressing cells (■).

3.2.3. RFP vs. GFP optical distortions

The effect of high optical density on the measurement of RFP-based sensors is compared with GFP-based sensors in Fig. 4 below. The same response surface methodology was applied to mCherry-based cells and the results indicate a greater immunity to optical distortions, as measured in the LED/LTF detector of this work.

4. Discussion

4.1. mCherry vs. GFP as reporters

Previous studies have compared various promoters and reporters side by side (Daunert et al., 2000; Hakkila et al., 2002; Justus and Thomas, 1999; Rettburg et al., 1999; Sagi et al., 2003; Shaner et al., 2005; Sörensen et al., 2003). No comparison appears to have been made using *mCherry* as a fluorescent reporter, despite its excellent properties as a reporter and tag (Shaner et al., 2005) and the suggestions that RFPs offer considerable advantages for whole-cell systems (Bartolome et al., 2006; Shrestha and Deo, 2006).

The performance of *recA::reporter* fusions on medium-copy plasmids in *E. coli* hosts was characterized in a miniature flow-through fluorometer in this study. RFP offers increased sensitivity and a lower limit of detection, when compared to GFP, using the methods of this study. It is tempting to attribute the improved performance to the optical properties of a red fluorophore. These properties include a greater transmissivity through dense cell media and higher LTF detector sensitivity to red wavelengths. From a brightness perspective, mCherry exhibits an extinction coefficient of 72,000 $M^{-1}\,cm^{-1}$ and quantum yield of 0.22 resulting in a relative brightness of 15,840 $M^{-1}\,cm^{-1}$ (Shaner et al., 2005). This is somewhat less than the approximate relative brightness of 19,800 $M^{-1}\,cm^{-1}$ of GFPmut3.1 (Arun et al., 2004; Cormack et al., 1996).

Biological factors may be involved in the better performance of *mCherry* over *gfpmut3.1*. For example, the half-life of mCherry protein has not been considered in this work, nor the protein's translational characteristics in comparison to GFPmut3.1. mCherry could simply be accumulating in higher quantities within the biosensor cells, resulting in better detection. It would be informative to biochemically quantify the two reporters.

Another possible explanation of the performance differences could simply be that the red fluorescence channel was more successfully executed than the green fluorescence channel, in terms of filter sets, LEDs, and the hand-painted apertures. Dye controls with matched spectral properties could potentially be performed to address this issue. Here, it suffices to say that *mcherry* outshines *gfpmut3.1* for the whole-cell assays conducted in the close-coupled, LTF photodiode-based detectors of this work.

For reference purposes, a commercial microplate spectrophotometer was used in parallel with the miniature detector of this work for GFP and RFP constructs (data not shown). In all cases, the commercial instrument exhibited a higher sensitivity, as defined by the change in fluorescence induction per change in genotoxin concentration. However, when the signal to noise ratios of the two instruments were compared, the LTF PD-based system performed comparably to (in the case of GFP) or in some cases better than (in the case of RFP) the commercial instrument under high-cell density conditions.

4.2. Comparison of interactions model and specific fluorescence model

High cell density optical assays are in general avoided since non-linear character emerges which complicates or confounds analysis. However, given the hardware complexity associated with automated sample preparation, methods which overcome high-thickness issues can be desirable for remote sensing applications.

Two related problems are associated with high-density optical measurement approaches. The first is that the true response of the cellular system is distorted. This is relevant when absolute terms are used in discussions. For example, fluorescent protein production models are often used to study gene expression. Those models are often crafted to account for the number of fluorophore molecules, and model parameters are derived from optical monitoring of progressing experiments. If distortions are present but not accounted for, then of course the models will be inaccurate. The second problem is that high-density optical measurements suffer from an inner-filter or self-shading effect. When the magnitude of the fluorescence response is used to establish detection criteria, dense samples underestimate the strength of the fluorescence response.

The result of the two-equation calibration effort in this work is to estimate the relative number of fluorophores in a sample rather than to quantify the amount of fluorescence observed. It should be noted that the calibrations were performed using mixtures of constitutive cells and cells with no fluorescent protein production. The assumption that 50% constitutive cells emit the same light as all cells expressing half the fluorescence of constitutive cells is probably not accurate and should be investigated further.

The calibration method presented here overcomes high-density sample distortions, but the improved accuracy comes at the cost of increased noise. Thus, for whole-cell biosensor applications based on signal to noise ratio detection criteria, calibrated and compensated fluorescence measurements are not superior to simple OD-normalizations. Thus, the bulk of this work with *recA::mCherry* biosensors does not rely on transformed measurements.

For other objectives, such as dynamic modeling or assessing the performance of engineered regulatory systems, the more complicated analysis presented here may be beneficial. This is more important for GFP than for RFP, as the green wavelengths are more susceptible to distortion than the reds.

4.3. MMC limit of detection

The *recA* promoter has been well-studied and characterized, and our data presented here, though obtained via simplified and more economical instrumentation, corresponds qualitatively to previously published material (see Table 2). Norman and co-workers reported a 9 nM MMC limit of detection using a PMT and the 2-fold

Table 2
MMC detection limits of genotoxicity tests.

Test	Limit (nM)	Modality	Reference
Ames test	0.2*	CFU count	Ptitsyn et al. (1997)
SOS-*lux* test	5	*cda::lux*	Ptitsyn et al. (1997)
SOS-*gfp* test	9	*cda::gfpmut3*	Norman et al. (2005)
SOS-*rfp* test	11.7	*recA::mcherry*	This work
SOS-*gfp* test	30	*recA::gfpmut3*	Sagi et al. (2003)
SOS-*gfp* test	115	*recA::gfpmut3.1*	This work

Limits of detection are presented based on the 2-fold fluorescence induction criteria.
* Ames test results based on a 2-fold increase in mutational events (over baseline).

induction criterion (and a more responsive promoter). Sagi and coworkers, using the same promoter as in this work, achieved a 30 nM MMC detection limit also using a PMT-based detector and the 2-fold induction criterion. Note that GFPmut3.1 refers to the commercially available reporter with the mut3 mutations (Cormack et al., 1996) and thus the reporters are substantially equivalent. For reference, a bioluminescence-based assay is tabulated as well, showing a 5 nM limit of detection also by the 2-fold induction criterion as measured by a PMT. Bioluminescence-based assays are generally reported as more sensitive than fluorescence-based assays, yet the work with *recA::mcherry* presented here approaches the same sensitivity. Also for reference is presented the classic Ames test, based on the frequency of mutational events as observed through the appearance of colony-forming units (CFUs). The Ames test, though available for many years now (Ames et al., 1973), still boasts the best limit of detection. Note that the limits of detection for the constructs in this work are reported according to the 2-fold induction criterion; much better limits can be reported using the SNR of 3 criterion. It is expected that the other constructs tested by the other investigators would also be much more sensitive had an SNR of 3 criterion been applied. It is worth noting that the *recA::mcherry* construct of this work achieves a limit of detection of about 0.25 nM when using the SNR of 3 criterion, making it potentially competitive with the Ames test from a limit of detection standpoint.

In practice, obtaining reference samples from the same parent CFU (such as is required to compute the induction factor) is not convenient and in some cases it is quite impossible. In these cases, a correlation of the raw fluorescence to optical density of a collection of MMC-treated cells can be used to estimate the MMC-treatment of a single sample without any control samples in the field. In this case, the limit of detection will suffer due to repeatability issues including optical instabilities (aging of LEDs, alignment of optical components, fouling of windows, etc.) or biological sources (altered tolerance to high reporter expression, mutations to fluorophores, etc.). Nevertheless, when a master curve fit was applied to the experiments of this study for *recA::mCherry* response to MMC treatments, dependable estimation of MMC concentration down to 10 nM was still easily achievable over a 4-month period (and swapping out of one of the LEDs).

5. Conclusion

A simple optical system based on close coupling of LEDs, PDs, filters, and sample chamber offers sufficient performance capabilities to make fluorescence measurements on whole-cell biosensors. In the developed system which is based on red-sensitive photodiodes, *recA::mCherry* constructs outperform *recA::gfpmut3.1* constructs for MMC detection in DJ480 cells. Using a fluorescence induction criterion for limit of detection assessment, the mCherry construct of this work as detected in the miniature optical system performs comparably to GFP-based sensors using bench-top PMTs as reported in the literature. When a signal to noise ratio of 3 was used as the criterion for limit of detection assessment, the *recA::mCherry* construct enables detection of MMC concentrations as low as 0.25 nM. By either criterion, RFP limits of detection as measured by the optical system in this work are superior to GFP limits by a factor of about 10.

The results presented in this work are similar to those reported for other systems, except that the instrument is amenable to portable, remote applications. The low-cost and simple nature of the optical system suggests the potential for multi-channel experiments with various sensor strains, highly distributed sensing, or disposable sensing.

Although the work performed herein was targeted toward MMC sensitivity, it is worth emphasizing that a large array of analytes is possibly investigated in this platform, as cited in the Section 1. For any analyte to which an inducible promoter has been identified, the possibility of implementation of a portable assay in this format exists. Furthermore, the optical cell developed herein is not restricted to use on *E. coli*-based assays. Any micro-organism or cell/cell component that can be placed even temporarily into liquid suspension could be harnessed for its sensing power. Indeed, for sampling techniques that result in irreproducible suspension concentrations (such as perhaps trypsinization of adherent cells), the concurrent estimation of biomass concentration and analyte-specific fluorescence could be potentially quite powerful.

Acknowledgments

This work was supported byNASA under grant NAG9#1359. This grant provided funding but did not provide other support in terms of experimental design, analysis, or reporting.

Appendix A. Supplementary data

Supplementary data associated with this article can be found, in the online version, at doi:10.1016/j.bios.2009.08.042.

References

Amann, E., Ochs, B., Abel, K.-J., 1988. Gene 69, 301–315.
Ames, B.N., Lee, F.D., Durston, W.E., 1973. Proc. Natl. Acad. Sci. 70, 782–786.
Arun, K.H.S., Kaul, C.L., Ramarao, P., 2004. J. Pharmacol. Toxicol. Methods 51, 1–23.
Bartolome, A.J., Mandap, K., David, K.J., Sevilla, F.I., Villanueva, J., 2006. Biosens. Bioelectron. 21, 2114–2120.
Baumstark-Khan, C., Rode, A., Rettburg, P., Horneck, G., 2001. Anal. Chim. Acta. 437, 23–30.
Belkin, S., 2003. Curr. Opin. Microbiol. 6, 206–212.
Bevis, B.J., Glick, B.S., 2002. Nat. Biotechnol. 20, 83–87.
Bulich, A.A., Huynh, H., Ulitzer, S., 1996. In: Ostrander, G.K. (Ed.), Techniques in Aquatic Toxicology. CRC Press, Inc..
Campbell, R.E., Tour, O., Palmer, A.E., Steinbach, P.A., Baird, G.S., Zacharias, D.A., Tsien, R.Y., 2002. Proc. Natl. Acad. Sci. 99, 7877–7882.
Cormack, B.P., Valdivia, R.H., Falkow, S., 1996. Gene. 173, 33–38.
Dasgupta, P.K., Eom, I.-Y., Morris, K., Li, J., 2003. Anal. Chim. Acta. 500, 337–364.
Daunert, S., Barrett, G., Feliciano, J.S., Shetty, R.S., Shrestha, S., Smith-Spencer, W., 2000. Chem. Rev. 100, 2705–2738.
Gotz, S., Karst, U., 2006. Anal. Bioanal. Chem. 387, 183–192.
Gu, M.B., Gil, G.C., 2001. Biosens. Bioelectron. 16, 661–666.
Hakkila, K., Maksimow, M., Karp, M., Virta, M., 2002. Anal. Biochem. 301, 235–242.
Justus, T., Thomas, S.M., 1999. Mutagenesis 14, 351–356.
King, J.M.H., Digrazia, P.M., Applegate, B.M., Burlage, R., Sanseverino, J., Dunbar, P., Larimer, F., Sayler, G.S., 1990. Science 249, 778–781.
Kostrzynska, M., Leung, K.T., Lee, H., Trevors, J.T., 2002. J. Microbiol. Methods 48, 43–51.
Kuang, Y., Biran, I., Walt, D.R., 2004. Anal. Chem. 76, 2902–2909.
LaRossa, R.A., Van Dyk, T.K., 2000. In: Storz, G., Hengge-Aronis, R. (Eds.), Bacterial Stress Responses. ASM Press, Washington, D.C..
Lee, J.H., Mitchell, R.J., Kim, B.C., Cullen, D.C., Gu, M.B., 2005. Biosens. Bioelectron. 21, 500–507.
Lei, Y., Chen, W., Mulchandani, A., 2006. Anal. Chim. Acta. 568, 200–210.
Majdalani, N., Heck, M., Stout, V., Gottesman, S., 2005. J. Bacteriol. 187, 6770–6778.
Montgomery, D.C., 2005. Design and Analysis of Experiments, 6th ed. John Wiley & Sons, Inc., Hoboken, NJ.
Norman, A., Hansen, L.H., Sørensen, S.J., 2005. Appl. Environ. Microbiol. 71, 2338–2346.
Paborji, M., Bogardus, J.B., Agharkar, S.N., Coppola, W.P., 1993. Stable solutions of mitomycin C. 5,216,011.

Ptitsyn, L.R., Horneck, G., Komova, O., Kozubek, S., Krasavin, E.A., Bonev, M., Rettburg, P., 1997. A biosensor for environmental genotoxin screening based on an SOS lux assay in recombinant *Escherichia coli* cells. Appl. Environ. Microbiol. 63, 4377–4384.
Polyak, B., Bassis, E., Novodvorets, A., Belkin, S., Marks, R.S., 2001. Sens. Actuators B. 74, 18–26.
Quillardet, P., Huisman, O., D'ari, R., Hofnung, M., 1982. Proc. Natl. Acad. Sci. 79, 5971–5975.
Rabbow, E., Rettburg, P., Baumstark-Khan, C., Horneck, G., 2003. Adv. Space Res. 31, 1513–1524.
Rettburg, P., Baumstark-Khan, C., Bandel, K., Ptitsyn, L.R., Horneck, G., 1999. Anal. Chim. Acta. 387, 289–296.
Ron, E.Z., 2007. Curr. Opin. Microbiol. 18, 252–256.
Sagi, E., Hever, N., Rosen, R., Bartolome, A.J., Premkumar, J.R., Ulber, R., Lev, O., Scheper, T., Belkin, S., 2003. Sens. Actuators B. 90, 2–8.
Shaner, N.C., Campbell, R.E., Steinbach, P.A., Giepmans, B.N.G., Palmer, A.E., Tsien, R.Y., 2004. Nat. Biotechnol. 22, 1567–1572.
Shaner, N.C., Steinbach, P.A., Tsien, R.Y., 2005. Nat. Methods 2, 905–909.
Shrestha, S., Deo, S.K., 2006. Anal. Bioanal. Chem. 386, 515–524.
Simpson, M.L., Sayler, G.S., Applegate, B.M., Ripp, S., Nivens, D.E., Paulus, M.J., Jellison, G.E.J., 1998. TIBTECH 16, 332–338.
Snyder, L., Champness, W., 2003. Molecular Genetics of Bacteria. ASM Press, Washington, D.C.
Sörensen, M., Lippuner, C., Kaiser, T., Mißlitz, A., Aebischer, T., Bumann, D., 2003. FEBS Lett. 552, 110–114.
Van Dyk, T.K., DeRose, E.J., Gonye, G.E., 2001. J. Bacteriol. 183, 5496–5505.
Wei, Y., Vollmer, A.C., LaRossa, R.A., 2001. J. Bacteriol. 183, 2259–2264.
Wiedenmann, J., Vallone, B., Renzi, F., Nienhaus, K., Ivanchenko, S., Rocker, C., Nienhaus, G.U., 2005. J. Biomed. Opt. 10, 14003.
Yagi, K., 2007. Appl. Microbiol. Biotechnol. 73, 1251–1258.